Original Article

www.ToxicolRes.org
Toxicological Research

Toxicol. Res. Vol. 35, No. 1, pp. 83-91 (2019)
https://doi.org/10.5487/TR.2019.35.1.083

Open Access

Zinc Oxide Nanoparticles Exhibit Both Cyclooxygenase- and Lipoxygenase-Mediated Apoptosis in Human Bone Marrow-Derived Mesenchymal Stem Cells

Dong-Yung Kim[1], Jun-Hyung Kim[1], Jae-Chul Lee[2], Moo-Ho Won[2], Se-Ran Yang[3], Hyoung-Chun Kim[4] and Myung-Bok Wie[1]

[1]Department of Veterinary Toxicology, College of Veterinary Medicine and Institute of Veterinary Science, Kangwon National University, Chuncheon, Korea
[2]Department of Neurobiology, School of Medicine, Kangwon National University, Chuncheon, Korea
[3]Department of Thoracic and Cardiovascular Surgery, School of Medicine, Kangwon National University, Chuncheon, Korea
[4]Neuropsychopharmacology and Toxicology Program, College of Pharmacy, Kangwon National University, Chuncheon, Korea

Abstract

Nanoparticles (NPs) have been recognized as both useful tools and potentially toxic materials in various industrial and medicinal fields. Previously, we found that zinc oxide (ZnO) NPs that are neurotoxic to human dopaminergic neuroblastoma SH-SY5Y cells are mediated by lipoxygenase (LOX), not cyclooxygenase-2 (COX-2). Here, we examined whether human bone marrow-derived mesenchymal stem cells (MSCs), which are different from neuroblastoma cells, might exhibit COX-2- and/or LOX-dependent cytotoxicity of ZnO NPs. Additionally, changes in annexin V expression, caspase-3/7 activity, and mitochondrial membrane potential (MMP) induced by ZnO NPs and ZnO were compared at 12 hr and 24 hr after exposure using flow cytometry. Cytotoxicity was measured based on lactate dehydrogenase activity and confirmed by trypan blue staining. Rescue studies were executed using zinc or iron chelators. ZnO NPs and ZnO showed similar dose-dependent and significant cytotoxic effects at concentrations ≥ 15 μg/mL, in accordance with annexin V expression, caspase-3/7 activity, and MMP results. Human MSCs exhibited both COX-2 and LOX-mediated cytotoxicity after exposure to ZnO NPs, which was different from human neuroblastoma cells. Zinc and iron chelators significantly attenuated ZnO NPs-induced toxicity. Conclusively, these results suggest that ZnO NPs exhibit both COX-2- and LOX-mediated apoptosis by the participation of mitochondrial dysfunction in human MSC cultures.

Key words: Zinc oxide nanoparticles, Apoptosis, Lipoxygenase, Cyclooxygenase-2, Mitochondrial membrane potential

INTRODUCTION

Nanoparticles (NPs) have been widely utilized in biomedical applications and industrial products owing to their special physicochemical characteristics. Despite the multifaceted availability of nanomaterials, they have a potential toxicological risk that has been a health concern for a long time (1,2). Zinc as an endogenous essential metal is known to accelerate neuronal injury by inhibiting mitochondrial energy production associated with neurodegenerative diseases such as cerebral ischemia and Alzheimer's disease (3,4). Zinc oxide (ZnO) NPs have been extensively applied to cosmetics including sunscreens, pharmaceuticals, semiconductors, dental fillings, and food additives owing to their antibacterial, antifungal, and anti-corrosive properties (5-7). With the expanded use of ZnO NPs, there might be human health problems because of this inadvertent exposure to them (8,9). Several researchers have reported that ZnO NPs could accu-

Correspondence to: Myung-Bok Wie, Department of Veterinary Toxicology, College of Veterinary Medicine and Institute of Veterinary Science, Kangwon National University, Chuncheon 24341, Korea
E-mail: mbwie@kangwon.ac.kr

pISSN: 1976-8257 eISSN: 2234-2753

mulate and/or damage major internal organs including the central nervous system via several routes (10,11). Reactive oxygen species (ROS) generated by massive ionic zinc dissolved from ZnO NPs may be one of the important components that are cytotoxic to many types of cells (12-14).

Mesenchymal stem cells (MSCs) reside in various organs including the brain. They are well known to exhibit multipotent capabilities (15). Thus, many investigators have attempted to develop tissue regeneration methods using the multifunctional abilities of stem cells when tissue damage occurs (15,16). However, studies on the interrelationship between MSCs and ZnO NPs are rare. Previously, we reported that the overactivation of the lipoxygenase (LOX) enzyme is the key modulator in the inflammatory process compared to the cyclooxygenase-2 (COX-2) enzyme associated with ZnO NPs-induced neurotoxicity in human dopaminergic neuroblastoma SH-SY5Y cells (12). Accordingly, we are interested in determining whether LOX and COX-2 are critical enzymes involved in cytotoxicity induced by ZnO NPs in MSCs. Human bone marrow-derived MSCs could be considered another important target in the process of cell injury caused by ZnO NPs. Therefore, the purpose of the present study was to determine the toxic concentrations and differences in cytotoxicity between ZnO NPs and ZnO using MSC cultures.

MATERIALS AND METHODS

Chemicals. ZnO NP (Lot No.: D28X017, Cat. No. 44898, ZnO NanoGard®) was purchased from Alfa Aesar Co (Ward Hill, MA, USA). ZnO (< 5 μm, 99.9%, CAS 1314-13-2) was obtained from Sigma-Aldrich Co (St. Louis, MO, USA). The average particle size of ZnO NPs powder was 67 nm (40-100 nm). The range of the specific surface area was 16 m^2/g (10-25 m^2/g). Fetal bovine serum (FBS), penicillin-streptomycin, trypan blue solution, and Dulbecco's Modified Eagle Medium (DMEM) were purchased from Gibco Co (Grand Island, NY, USA). *N,N,N′,N′*-tetrakis-(2-pyridylmethyl) ethylenediamine (TPEN) was purchased from Enzo Life Sciences (Farmingdale, NY, USA). Esculetin, meloxicam, deferoxamine mesylate, 3-(4,5-dimethylthiazol-2-yl)-2,5-diphenyltetrazolium bromide, and $ZnCl_2$ were purchased from Sigma Chemical Co (St. Louis, MO, USA).

ZnO NPs and ZnO suspensions. ZnO NPs and ZnO suspensions were prepared with Millipore water at concentrations of 1 mg/mL. Before adding ZnO NPs or ZnO to the culture media, each suspension was sonicated for at least 20 min and vortexed vigorously. The suspension was then immediately applied to the cultured MSCs.

Cultures of MSCs and exposure to ZnO NPs or ZnO. Human bone marrow-derived MSCs were obtained from the Catholic Institute of Cell Therapy (CIC, Seoul, Korea). The present study was approved by the Kangwon National University Institutional Review Board (KWNUIRB-2016-03-002). MSCs were subcultured at a concentration of 5×10^4 cells/cm^2 in MSC growth medium (DMEM containing 10% FBS, 100 μg/mL streptomycin, and 100 U/mL penicillin). Cultured MSCs were used for experiments during passages 5 to 8. These cells were incubated in a humidified atmosphere at 37°C with 5% CO_2. Cells were harvested using 0.25% trypsin EDTA. They were subcultured into 100 mm dishes. Grown cells were seeded into 6-well and 24-well plates for various experiments. After 1 or 2 days, ZnO NPs, ZnO, and/or other compounds were added when the cell density was confluent at 70-80%.

Measurement of lactate dehydrogenase (LDH) activity. MSCs were seeded into 24-well plates at a cell density of 2×10^5 cells. These cells were then treated with different concentrations (10, 15, 20, and 30 μg/mL) of ZnO NPs or ZnO for 20-24 hr. After treatment, cell injury was quantitatively estimated by measuring the LDH released from damaged cells into the culture medium at 20-24 hr after ZnO NPs or ZnO exposure as described previously (17). LDH activity was measured at a wavelength of 340 nm using a kinetic program on a VersaMax Eliza Reader (Molecular Devices, San Jose, CA, USA).

Trypan blue exclusion test. To determine whether cells were viable or non-viable, MSCs were exposed to 0.4% trypan blue solution in culture media. After 5 min of exposure, cells were washed with HBSS three times and photographed by phase contrast (Sunny, Nahwoo Co., Suwon, Korea).

Annexin V and dead cell assay. Annexin V and dead cell assay were performed for quantitative analysis of live, early apoptosis, late apoptosis, and cell death. Stained cells were analyzed using an annexin V and dead cell kit (Catalog No. MCH100105, Merck, Darmstadt, Germany). Staining of dead cells used a 7-amino-actinomycin D (7-AAD) marker according to the instructions of the annexin V and dead cell kit. Briefly, after ZnO NPs or ZnO exposure for 12 hr or 24 hr, MSCs were harvested and resuspended in 1X assaying buffer to a density of 5×10^5 cells/mL. Annexin V reagent was then added to the cells and incubated for 20 min at room temperature. Percentages of death type were estimated using a Muse cell analyzer (Merck).

Caspase 3/7 activity assay. To examine caspase 3/7 activity, MSCs were plated onto 6-well plates at a density of 5×10^5 cells/well. After treatment with different concentrations (10, 15, 20, 25, and 30 μg/mL) of ZnO NPs or ZnO for 12 or 24 hr, caspase 3/7 activity was analyzed using a caspase 3/7 kit (Catalog No. MCH100108, Merck).

Briefly, cells were collected by trypsin EDTA. Then, 5 μL of Muse working solution was added to 50 μL of cells and incubated at 37°C for 30 min. After incubation, 150 μL of 7-AAD working solution was added. Cell suspensions were used to estimate the proportions of four cell populations, including percentages of live cells, apoptotic cells exhibiting caspase 3/7 activity, late apoptotic/dead cells, and necrotic cells according to the Muse cell analyzer protocol.

Measurement of mitochondrial membrane potential (MMP). MMP changes of cultured MSCs induced by ZnO NPs or ZnO were examined with a Muse cell analyzer (Merck). MMP was measured using a commercial Muse® Mitopotential assay kit (Merck). Briefly, cultured MSCs were harvested using trypsin EDTA and centrifuged at 300 × *g* for 5 min. Sedimented cells were resuspended in 1X assay buffer and mixed with Muse mitopotential reagent followed by incubation at 37°C for

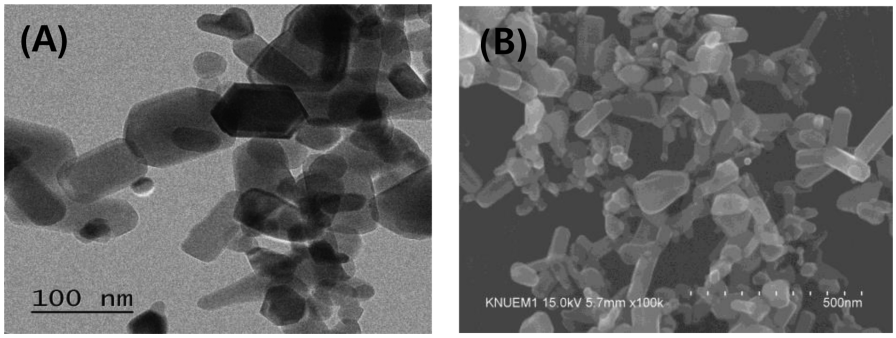

Fig. 1. Representative transmission electron microscope (A) and scanning electron microscope (B) images of zinc oxide nanoparticles (ZnO NPs). ZnO NPs aggregates are observed at higher magnification. Magnification: 100,000×.

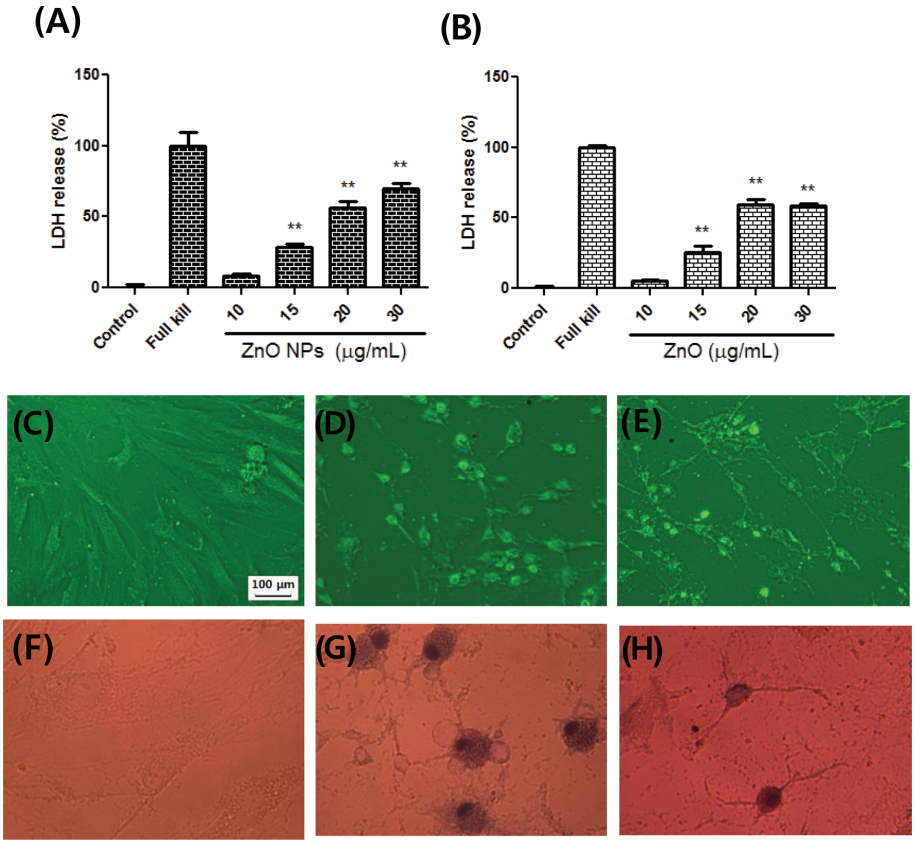

Fig. 2. Dose-toxicity effects of ZnO NPs (A) and ZnO (B) in mesenchymal stem cells (MSC) cultures. Cytotoxicity was evaluated by lactate dehydrogenase (LDH) release. Microscopic image of MSCs by phase contrast (C, D, E) or staining with trypan blue (F, G, H). (C, F) control; (D, G) 15 μg/mL ZnO NPs; (E, H) 15 μg/mL ZnO. $^{**}p < 0.01$ compared to the control (n = 4).

20 min. Then, 5 μL of 7-AAD reagent was added. Data were obtained following the protocol of the Muse cell analyzer.

Statistical analyses. All statistical analyses were performed using the SAS 9.4 software program and one-way analysis of variance Dunnett's test. Statistical significance was considered at $p < 0.05$. Experimental data are expressed as mean ± standard error of the mean (SEM).

RESULTS

Nanoparticle (NP) characterization. ZnO NPs were characterized using a field emission transmission electron microscope (FETEM, Model: JEM2100F, JEOL Co, Tokyo, Japan) (Fig. 1A). The accelerating condition was at 200 kV. Ultra-high resolution scanning electron microscope (S-4800, Hitachi, Ibaraki, Japan) images for ZnO NPs exhibited a rod-shaped and agglomerated morphology (Fig. 1B) at accelerating voltage of 15 kV and magnification of 100,000×.

Cytotoxicity of ZnO NPs and ZnO. Exposure of cultured human bone marrow-derived MSCs to ZnO NPs or ZnO (10, 15, 20, 25, and 30 μg/mL) resulted in cytotoxicity in a concentration-dependent fashion (Fig. 2A, 2B). Statistically significant cytotoxicity was observed after exposure to ZnO NPs or ZnO at concentrations ≥ 15 μg/mL.

Therefore, we executed rescue studies using several cytoprotective compounds against ZnO NPs-induced toxicity at a concentration of 15 μg/mL. Toxicity differences between ZnO NPs and ZnO measured by LDH activity were not observed. Phase contrast microscope imaging (Fig. 2C-2E) and trypan blue staining (Fig. 2F-2H) were performed for morphological and viability confirmation, respectively.

Effects of ZnO NPs or ZnO on annexin V and dead cell assay. The distribution of live, apoptosis and dead cells induced by ZnO NPs or ZnO was illustrated in Fig. 3A, 3B, 3C. Total apoptosis (annexin V) induced by ZnO NPs or ZnO exposure showed concentration-dependent elevation after 12 hr (Fig. 3B). Apoptotic injury at 12 hr after ≥ 15 μg/mL ZnO NPs or ZnO treatment was significantly

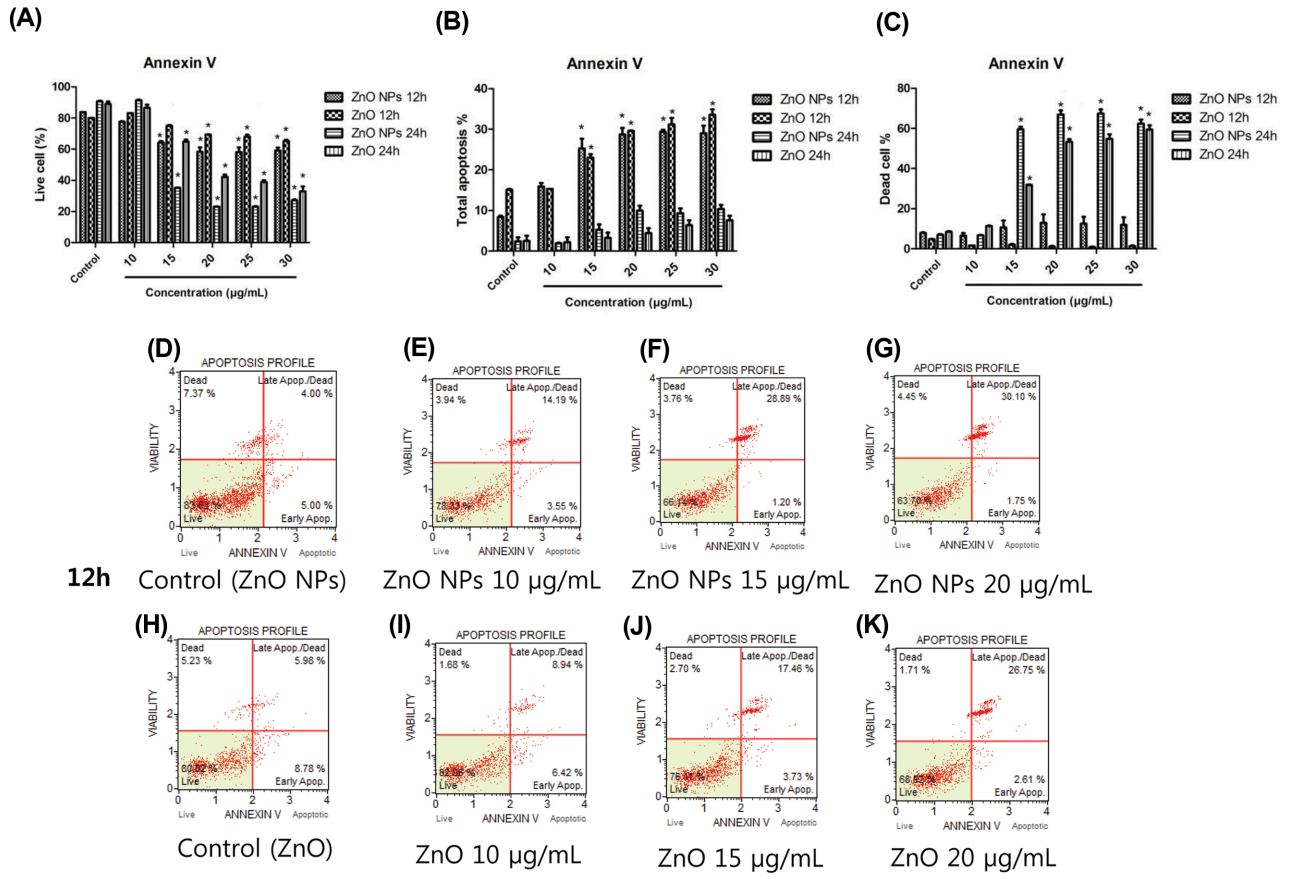

Fig. 3. Effects of ZnO NPs or ZnO on cultured MSCs based on Annexin V and dead cell assay at 12 hr or 24 hr after exposure. Profiles of live cell (A), total apoptosis (B), and dead cell (C) after exposure to different concentrations (0, 10, 15, 20, 25, and 30 μg/mL) of ZnO NPs or ZnO are illustrated. Representative flow cytometry data of ZnO NPs (D, E, F, G) and ZnO (H, I, J, K) at 12 hr after exposure to ZnO NPs or ZnO are shown. *$p < 0.05$ compared to the control (n = 4).

higher than that of the control. Generally, the total apoptosis ratio was not different between ZnO NPs and ZnO. Representative flow cytometry analysis results for MSCs at 12 hr after ZnO NPs or ZnO treatment are shown in Fig. 3D-3K.

Effects of ZnO NPs and ZnO on caspase-3/7 activity. Exposure of MSCs to ZnO NPs or ZnO (15-30 μg/mL) significantly altered caspase-3/7 activity at 12 hr and 24 hr after exposure (Fig. 4A-4C). However, differences in caspase-3/7 activity between ZnO NPs- and ZnO-treated groups did not show in all ranges of concentration except in 15 μg/mL.

Representative flow cytometry analysis results for MSCs at 12 hr after ZnO NP or ZnO treatment are shown in Fig. 4D-4K.

Effects of ZnO NPs and ZnO on mitochondrial membrane potential (MMP). Treatment of cultured MSCs with ZnO NPs showed significant reduction in the number of depolarized live cells and elevation in the number of depolarized dead cells at ≥ 15 μg/mL concentrations (Fig. 5A). Exposure of ZnO exhibited a similar pattern in depolarized dead cells similar to that of ZnO NPs (Fig. 5B). However, the mean value of depolarized dead cells in the ZnO NPs group was two-fold higher than that of ZnO at 15 μg/mL concentration (Fig. 5A, 5B). Representative flow cytometry analysis results for MMP measurement at 12 hr after ZnO NPs or ZnO treatment are shown in Fig. 5C-5J.

Protective effects of LOX and COX-2 inhibitors. Esculetin as a LOX inhibitor and meloxicam as a COX-2 inhibitor significantly attenuated ZnO NPs-induced cytotoxicity in MSC cultures (Fig. 6A, 6B). However, the LOX inhibitor showed much better protective effects than that of the COX-2 inhibitor. Morphological confirmation by trypan blue staining corresponded well with LDH results (Fig. 6C-6F).

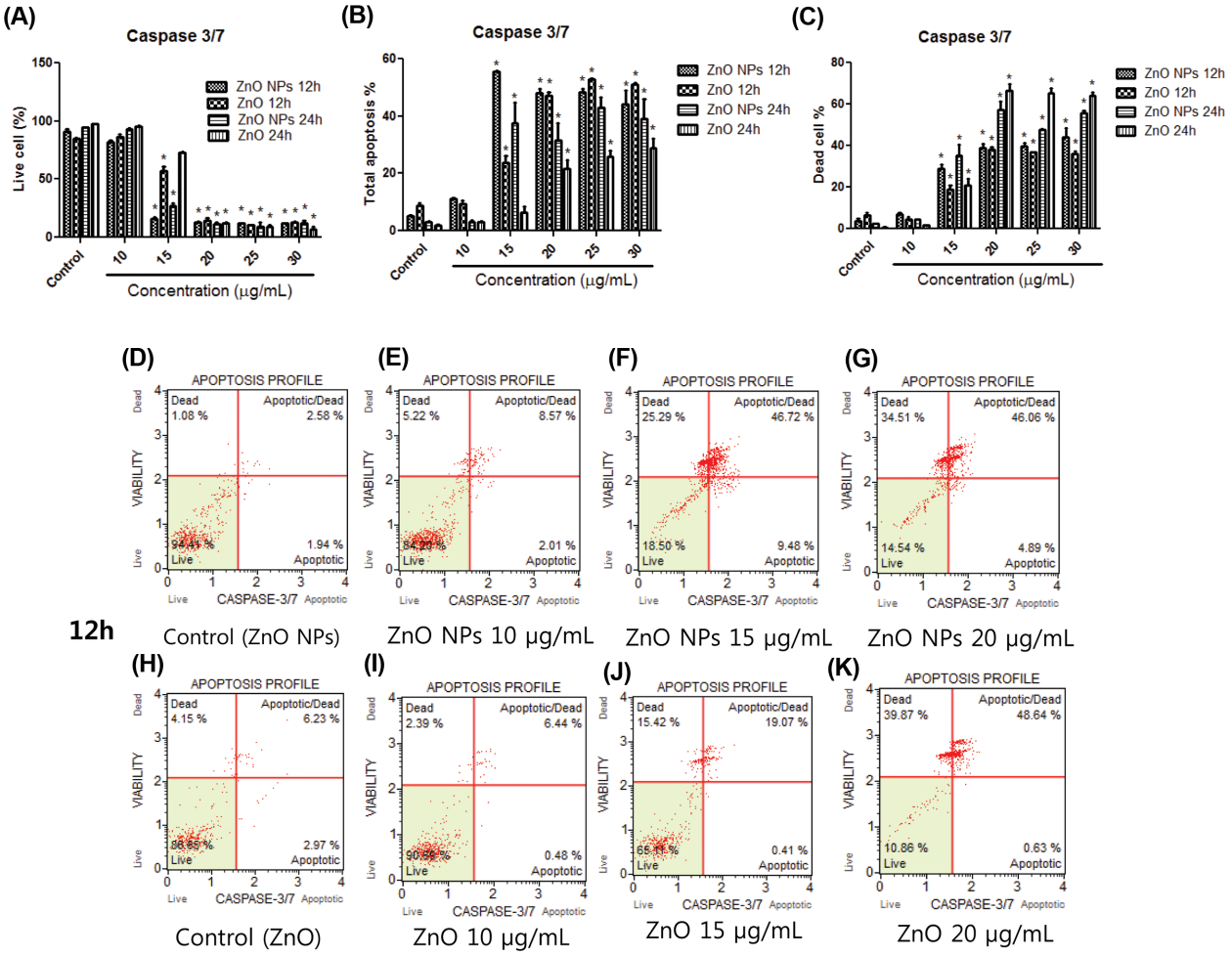

Fig. 4. Effects of ZnO NPs or ZnO on caspase 3/7 activity in cultured MSCs. Cell profiles of live cell (A), total apoptosis (B), and dead cell (C) are illustrated. Representative flow cytometry data of ZnO NPs (D, E, F, G) and ZnO (H, I, J, K) at 12 hr after exposure to ZnO NPs or ZnO are shown. *$p < 0.05$ compared to the control (n = 4).

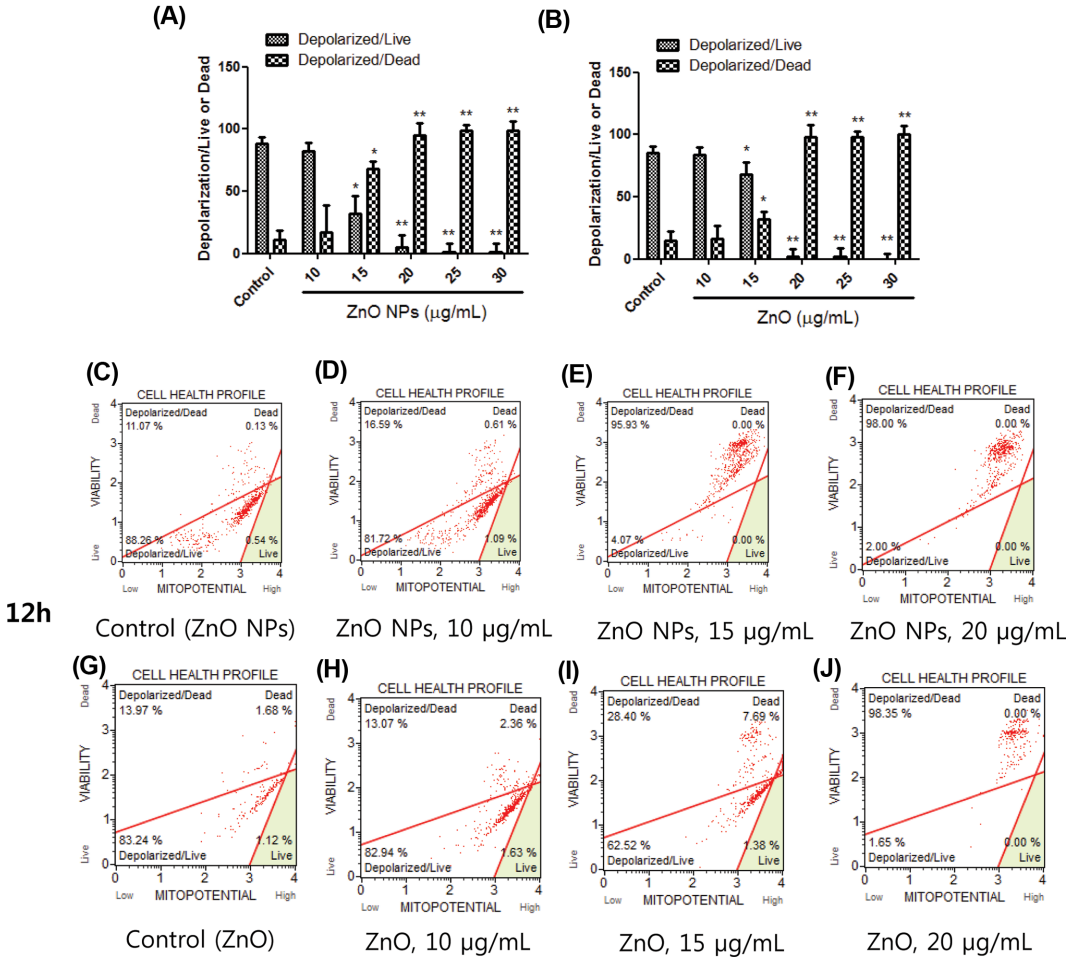

Fig. 5. Effects of ZnO NPs or ZnO on mitochondrial membrane potential (MMP) in cultured MSCs. The ratio of depolarized/live or depolarized/dead cells is illustrated (A, B). Representative flow cytometry data of ZnO NPs (C, D, E, F) and ZnO (G, H, I, J) at 12 hr after exposure to ZnO NPs or ZnO are shown. $*p < 0.05$, $**p < 0.01$ compared to the control (n = 4).

Protective effects of zinc or iron chelator against ZnO NP toxicity. TPEN as a membrane permeable zinc chelator and deferoxamine as an iron chelator significantly inhibited ZnO NPs-induced cytotoxicity in MSC cultures (Fig. 7A, 7B). Morphological confirmation by trypan blue staining corresponded with LDH results (Fig. 7C-7F).

DISCUSSION

In the present study, we found that the inhibitor of LOX or COX-2 significantly attenuated cytotoxicity induced by ZnO NPs in MSC cultures. In addition, esculetin as a LOX inhibitor showed a much better protective effect than that of meloxicam, which is a COX-2 inhibitor. These results suggest that arachidonic acid metabolism between human neuroblastoma cells and human MSCs during the inflammatory process induced by ZnO NPs could be different based on cell types. Van Rossum *et al.* (18) reported that LOX is involved in the progress of the cell cycle of neuroblastoma cells. Moreover, intracellular zinc could correlate with the elevation of LOX activity in neuronal death (19). In the present study, delayed cellular swelling was observed during the late stages of ZnO NP-induced toxicity in MSC cultures. We found that the significant toxic concentration of ZnO NPs in cultured MSCs was ≥ 15 μg/mL, in accordance with previous results (12,14,20). Several recent studies have suggested that different sized ZnO NPs exhibited similar cytotoxicity, with the median toxic dose being approximately 10-20 μg/mL (14,20). Similarly, our apoptotic results using annexin V and caspase-3/7 activity as well as MMP were significant at ≥ 15 μg/mL ZnO NPs and there was no significant difference between ZnO NPs and ZnO in cultured MSCs. These results suggest that the cytotoxicity of NPs is chiefly attributed to dissolved zinc ions, not the NP itself, by exposure to ZnO NPs (14). The zinc ion derived from ZnO NPs is known to mediate oxidative stress by causing dysfunction in mitochondrial respiration (21). After depleting ATP produc-

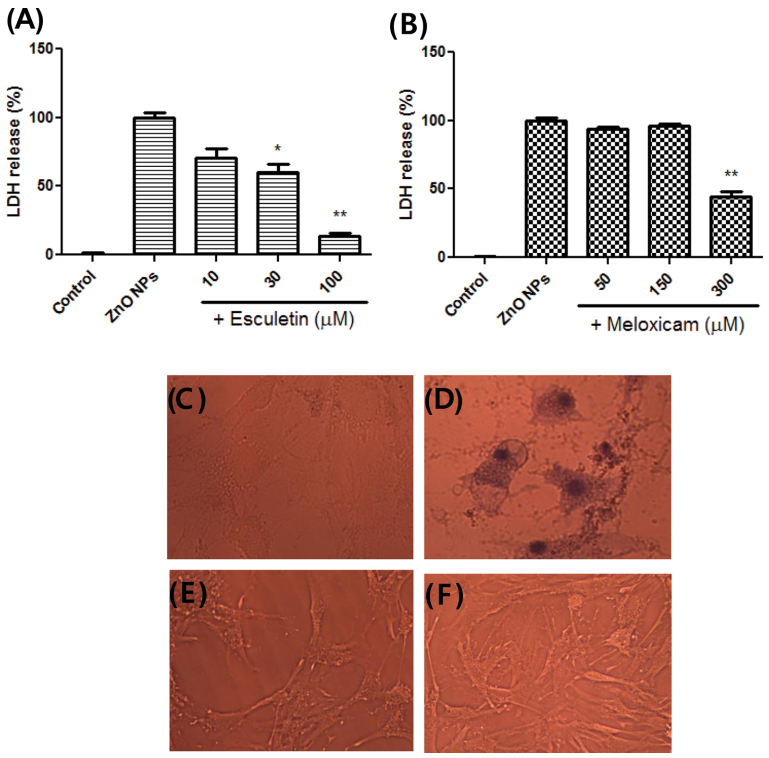

Fig. 6. Protective effects of esculetin (A) and meloxicam (B) against ZnO NP-induced cytotoxicity in MSC cultures. Cytotoxicity was evaluated by LDH release. Microscopic image of MSCs by staining with trypan blue (C, D, E, F). (C) control, (D) 15 μg/mL ZnO NPs, (E) 15 μg/mL ZnO NPs + 100 μM esculetin. (F) 15 μg/mL ZnO NPs + 300 μM meloxicam. *$p < 0.05$, **$p < 0.01$ compared to the control (n = 4).

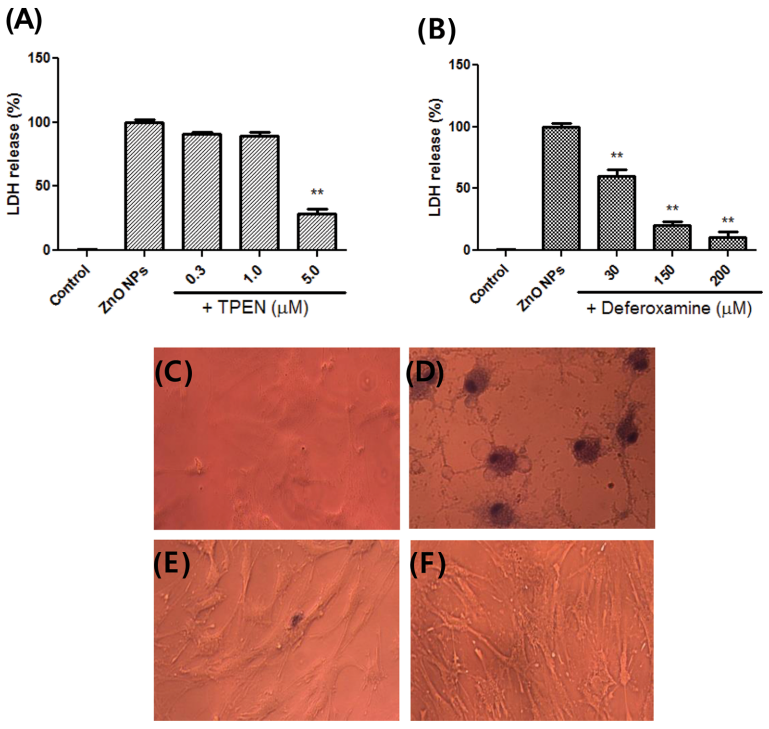

Fig. 7. Protective effects of TPEN, a zinc chelator (A) and deferoxamine, an iron chelator (B) against ZnO NP-induced toxicity in MSCs. Cytotoxicity was evaluated by LDH release. Microscopic image of MSCs by staining with trypan blue (C, D, E, F). (C) control, (D) 15 μg/mL ZnO NPs, (E) 15 μg/mL ZnO NPs + 5 μM TPEN. (F) 15 μg/mL ZnO NPs + 200 μM deferoxamine. **$p < 0.01$ compared to the control (n = 4).

tion by increasing free zinc dissolved from ZnO NPs, the release of cytochrome C, activation of caspase 3/7, and apoptosis serially occurs (3,22). TPEN as a membrane permeable specific zinc chelator and deferoxamine as an iron-specific chelator recovered the ZnO NPs-induced toxicity to a normal state. TPEN is also known to inhibit the activity of 12-LOX (19). Iron chelation by deferoxamine might contribute to the survival of human MSCs by suppressing the production of ROS via ZnO NPs-induced oxidative injury (23,24). These results suggest that metal chelators could be developed as a therapy or prevention for human neurodegenerative diseases or various cytotoxic diseases caused by metal-associated NPs (25,26). Although nanotoxicity studies caused by ZnO NPs in human or animal MSCs are gradually increasing, the exact mechanism involved in such nanotoxicity has not been clearly clarified to date (27,28). NPs appear to show diverse physicochemical alterations or responses in accordance with the exposed microenvironment in various *in vitro* or *in vivo* systems (29). Consequently, cytotoxicity induced by ZnO NPs might involve the simultaneous activation of COX-2 and LOX enzymes including caspase 3/7-mediated apoptosis by mitochondrial dysfunction in cultured MSCs.

ACKNOWLEDGMENTS

This study was supported by the 2015 Research Grant from Kangwon National University (No. 520150277).

CONFLICT OF INTEREST

The authors declare that they have no conflicts of interest to disclose.

Received July 16, 2018; Revised August 16, 2018; Accepted August 30, 2018

REFERENCES

1. Navya, P.N. and Daima, H.K. (2016) Rational engineering of physicochemical properties of nanomaterials for biochemical applications with nanotoxicological perspectives. *Nano. Converg.*, **3**, 1-14.
2. Wu, T. and Tang, M. (2018) Review of the effects of manufactured nanoparticles on mammalian target organs. *J. Appl. Toxicol*., **38**, 25-40.
3. Dineley, K.E., Votyakova, T.V. and Reynolds, I.J. (2003) Zinc inhibition of cellular energy production: implication for mitochondria and neurodegeneration. *J. Neurochem*., **85**, 563-570.
4. Capasso, M., Jeng, J.M., Malavolta, M., Mocchegiani, E. and Sensi, S.L. (2005) Zinc dyshomeostasis: a key modulator of neuronal injury. *J. Alzheimers Dis*., **8**, 93-108.
5. Manzoor, U., Siddique, S., Ahmed, R., Noreen, Z., Bokhari, H. and Ahmed, I. (2016) Antibacterial, structural and optical characterization of mechano-chemically prepared ZnO nanoparticles. *PLoS ONE*, **11**, e0154704.
6. Sardella, D., Gatt, R. and Valdramidis, V.P. (2017) Physiological effects and mode of action of ZnO nanoparticles against postharvest fungal contaminants. *Food Res. Int*., **101**, 274-279.
7. Hosseini, M., Fotouhi, L., Ehsani, A. and Naseri, M. (2017) Enhancement of corrosion resistance of polypyrrole using metal oxide nanoparticles: potentiodynamic and electrochemical impedance spectroscopy study. *J. Colloid Interface Sci.*, **505**, 213-219.
8. Kim, Y.H., Kwak, K.A., Kim, T.S., Seok, J.H., Roh, H.S., Lee, J.K., Jeong, J., Meang, E.H., Hong, J.S., Lee, Y.S. and Kang, J.S. (2015) Retinopathy induced by zinc oxide nanoparticles in rats assessed by micro-computed tomography and histopathology. *Toxicol. Res*., **31**, 157-163.
9. Kim, K.B., Kim, Y.W., Lim, S.K., Roh, T.H., Bang, D.Y., Choi, S.M., Lim, D.S., Kim, Y.J., Baek, S.H., Kim, M.K., Seo, H.S., Kim, M.H., Kim, H.S., Lee, J.Y., Kacew, S. and Lee, B.M. (2017) Risk assessment of zinc oxide, a cosmetic ingredient used as a UV filter of sunscreens. *J. Toxicol. Environ. Health B Crit. Rev.*, **20**, 155-182.
10. Kao, Y.Y., Cheng, T.J., Yang, D.M., Wang, C.T., Chiung, Y.M. and Liu, P.S. (2012) Demonstration of an olfactory bulb-brain translocation pathway for ZnO nanoparticles in rodent cells in vitro and in vivo. *J. Mol. Neurosci*., **48**, 464-471.
11. Tian, L., Lin, B., Wu, L., Li, K., Liu, H., Yan, J., Liu, X. and Xi, Z. (2015) Neurotoxicity induced by zinc oxide nanoparticles: age-related differences and interaction. *Sci. Rep*., **5**, 16117-16129.
12. Kim, J.H., Jeong, M.S., Kim, D.Y., Her, S. and Wie, M.B. (2015) Zinc oxide nanoparticles induce lipoxygenase-mediated apoptosis and necrosis in human neuroblastoma SH-SY5Y cells. *Neurochem. Int*., **90**, 204-214.
13. Heim, J., Felder, E., Tahir, M.N., Kaltbeizel, A., Heinrich, U.R., Brochhausen, C., Mailander, V., Tremel, W. and Brieger, J. (2015) Genotoxic effects of zinc oxide nanoparticles. *Nanoscale*, **7**, 8931-8938.
14. Song, W., Zhang, J., Guo, J., Zhang, J., Ding, F., Li, L. and Sun, Z. (2010) Role of the dissolved zinc ion and reactive oxygen species in cytotoxicity of ZnO nanoparticles. *Toxicol. Lett*., **199**, 389-397.
15. Mohr, A. and Zwacka, R. (2018) The future of mesenchymal stem cell-based therapeutic approaches for cancer-From cells to ghosts. *Cancer Lett*., **414**, 239-249.
16. Spees, J.L., Lee, R.H. and Gregory, C.A. (2016) Mechanisms of mesenchymal stem/stromal cell function. *Stem Cell Res. Ther*., **7**, 125-138.
17. Koh, J.Y. and Choi, D.W. (1987) Quantitative determination of glutamate-mediated cortical neuronal injury in cell culture by lactate dehydrogenase efflux assay. *J. Neurosci. Methods*, **20**, 83-90.
18. van Rossum, G.S., Bijvelt, J.J., van den Bosch, H., Verkleij, A.J. and Boonstra, J. (2002) Cytosolic phospholipase A2 and lipoxygenase are involved in cell cycle progression in neuroblastoma cells. *Cell Mol. Life Sci*., **59**, 181-188.
19. Zhang, Y., Aizenman, E., DeFranco, D.B. and Rosenberg, P.A. (2007) Intracellular zinc release, 12-lipoxygenase acti-

vation and MAPK dependent neuronal and oligodendroglial death. *Mol. Med*., **13**, 350-355.
20. Deng, X., Luan, Q., Chen, W., Wang, Y., Wu, M., Zhang, H. and Jiao, Z. (2009) Nanosized zinc oxide particles induce neural stem cell apoptosis. *Nanotechnology*, **20**, 115101.
21. Wang, J., Deng, X., Zhang, F., Chen, D. and Ding, W. (2014) ZnO nanoparticle-induced oxidative stress triggers apoptosis by activating JNK signaling pathway in cultured primary astrocyte. *Nanoscale Res. Lett*., **9**, 117-129.
22. Yu, K.N., Yoon, T.J., Minai-Tehrani, A., Kim, J.E., Park, S.J., Jeong, M.S., Ha, S.W., Lee, J.K., Kim, J.S. and Cho, M.H. (2013) Zinc oxide nanoparticle induced autophagic cell death and mitochondrial damage via reactive oxygen species generation. *Toxicol. In Vitro*, **27**, 1187-1195.
23. Armstrong, C., Leong, W. and Lees, G.J. (2001) Comparative effects of metal chelating agents on the neuronal cytotoxicity by copper (Cu^{2+}), iron (Fe^{3+}) and zinc in the hippocampus. *Brian Res.*, **892**, 51-62.
24. Sharma, V., Anderson, D. and Dhawan, A. (2012) Zinc oxide nanoparticles induce oxidative DNA damage and ROS-triggered mitochondria mediated apoptosis in human liver cells (HepG2). *Apoptosis*, **17**, 852-870.
25. Liu, G., Men, P., Perry, G. and Smith, M.A. (2010) Nanoparticle and iron chelators as a potential novel Alzheimer therapy. *Methods Mol. Biol*., **610**, 123-144.
26. Wang, N., Jin, X., Guo, D., Tong, G. and Zhu, X. (2017) Iron chelation nanoparticles with delayed saturation as an effective therapy for Parkinson Disease. *Biomacromolecules*, **18**, 461-474.
27. Ickrath, P., Wagner, M., Scherzad, A., Burgahartz, M., Hagen, R., Kleinsasser, N. and Hackenberg, S. (2017) Time-dependent toxic and genotoxic effects of zinc oxide nanoparticles after long-term and repetitive exposure to human mesenchymal stem cells. *Int. J. Environ. Res. Public Health*, **14**, E1590.
28. Syama, S., Sreekanth, P.J., Varma, H.K. and Mohanan, P.V. (2014) Zinc oxide nanoparticles induced oxidative stress in mouse bone marrow mesenchymal stem cells. *Toxicol. Mech. Methods*, **24**, 644-653.
29. Zhang, X., Li, W. and Yang, Z. (2015) Toxicology of nanosized titanium oxide: an update. *Arch. Toxicol*., **89**, 2207-2217.